

Recursion method for nonhomogeneous superconductors: Proximity effect in superconductor-ferromagnet nanostructures

E. Vecino, A. Martín-Rodero, and A. Levy Yeyati

Departamento de Física Teórica de la Materia Condensada C-V, Universidad Autónoma de Madrid, E-28049 Madrid, Spain

(Received 11 June 2001; published 9 October 2001)

We present a theoretical method to study the electronic local spectral density of hybrid nanostructures consisting of a normal (N) or ferromagnetic (F) region deposited on top of a superconductor (S). Our approach is based on a lattice Hamiltonian model which allows to describe the spatial variation of the superconducting order parameter in nanostructures of arbitrary geometry. In order to obtain the local density of states we develop a generalization of the recursion method valid for systems containing superconducting and ferromagnetic regions. As a first step we analyze the proximity effect and the detailed behavior of Andreev states in one-dimensional (1D) N - S and F - S structures. We study the transition from the 1D case to the limit of infinite lateral dimensions in the ballistic regime. Finally we analyze the spatial variation of the proximity effect as a function of the exchange field in F - S nanostructures. It is found that the oscillations in the induced pairing amplitude in the scale of the ferromagnetic coherence length can be correlated to the crossing of Andreev states through the Fermi energy as a function of the ferromagnetic region size.

DOI: 10.1103/PhysRevB.64.184502

PACS number(s): 74.50.+r, 74.80.-g, 75.70.-i

I. INTRODUCTION

A normal metal (N) in good contact with a superconductor (S) is known to acquire superconducting properties in a region close to the interface. This effect, known as the proximity effect, has been extensively studied for more than 30 years.¹ With the development of nanofabrication techniques it has become possible to analyze the proximity effect with spatial resolution in the mesoscopic regime² which has stimulated a renewed interest in more detailed theories. On the other hand, the proximity effect in ferromagnets (F) has remained so far a less understood phenomenon. Many recent experiments have been conducted in order to test the proximity effect on F - S structures.³⁻⁶ Some of these experiments seem to be in contradiction with the general “wisdom” stating that superconducting correlations should be destroyed beyond distances of the order of $\xi_F = \hbar v_F / \pi E_{\text{ex}}$, where E_{ex} is the exchange field in the ferromagnet, which is of the order of a few nanometers in usual ferromagnets. On the theoretical side, the proximity effect has been mainly analyzed using the Usadel equations⁷ for semiclassical Green functions. This approach has allowed a rather complete understanding of the proximity effect in normal diffusive conductors. However, actual nanostructures with typical dimensions of the order or smaller than the elastic mean free path can be closer to a ballistic situation.⁸ Further theoretical developments covering the range between diffusive and ballistic regimes are thus desirable. At the same time, the theory should be able to account for geometrical effects that can be relevant in real nanostructures.

To get a microscopic insight it is convenient to start from a model Hamiltonian incorporating the essential physical ingredients. For the description of nonhomogeneous systems it is useful to formulate this model using a local orbital basis. This type of approach has been introduced in the context of superconductivity in Refs. 9,10 and is specially well suited to analyze transport properties when a detailed description of the geometry is needed. This approach naturally allows for a self-consistent determination of the spatial variation of the

order parameter¹⁰ and to incorporate electron-correlation effects.¹¹ Furthermore, itinerant magnetism has been traditionally analyzed by means of model Hamiltonians written in a local representation such as the Hubbard model or its many extensions.¹² These lattice models thus provide an adequate framework for a more microscopic description of the interplay between superconductivity and ferromagnetism in actual nanostructures.

On the other hand, the recursion method introduced by Haydock *et al.*¹³ for the evaluation of the local density of states in normal systems is a powerful computational tool,¹⁴ particularly suitable to analyze systems with an arbitrary geometry as it does not rely on translational symmetry assumptions. It is thus desirable to extend this method to situations where superconducting correlations are present. Although some attempts in this direction have already been made¹⁵ further developments seem to be necessary, specially for dealing with the combination of superconductors and ferromagnets.

The aim of the present work is twofold: first, we introduce a generalization of the recursion method for the case of hybrid N - S and F - S structures. Secondly, we use this method to study the proximity effect in the ballistic limit for different geometries in N - S and F - S structures.

The paper is organized as follows. In Sec. II we introduce the microscopic model. Section III is devoted to the analysis of the quasiparticle spectrum of one-dimensional models for N - S and F - S structures. In Sec. IV we discuss the generalization of the recursion method for the calculation of local Green functions in N - S or F - S structures. In Sec. V we present results for different 3D N - S and F - S nanostructures which illustrate the behavior of the induced pairing amplitude and local densities of states for different geometries. The conclusions are finally presented in Sec. VI.

II. THE MICROSCOPIC MODEL

In the present work we analyze the proximity effect in different hybrid nanostructures such as the one depicted in

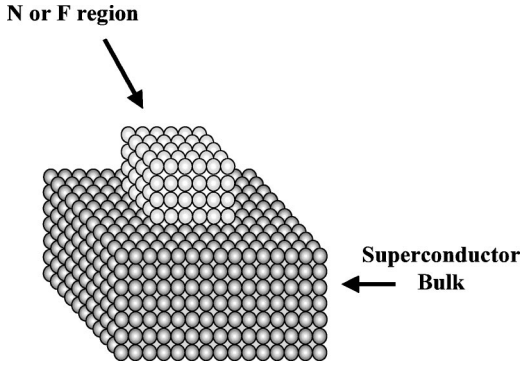
FIG. 1. Typical geometry for a hybrid $N(F)$ - S nanostructure.

Fig. 1. For describing the electronic states in such systems we introduce a model Hamiltonian in a local representation which, for a ferromagnetic region, adopts the form

$$\hat{H}_F = \sum_{i,\sigma} (\epsilon_{i,\sigma} - \mu) c_{i\sigma}^\dagger c_{i\sigma} + \sum_{i \neq j, \sigma} t_{ij} c_{i\sigma}^\dagger c_{j\sigma}, \quad (1)$$

where i, j run over the different sites of the system, t_{ij} are the hopping parameters connecting the different sites; μ is the chemical potential and $\epsilon_{i,\sigma}$ is a spin dependent site energy which can take into account the presence of an exchange field ($\epsilon_{i,\uparrow} - \epsilon_{i,\downarrow} = E_{\text{ex}}$). The Hamiltonian for a normal metal \hat{H}_N is simply recovered by making $E_{\text{ex}} = 0$. On the other hand, for the superconducting regions one has^{9,10}

$$\begin{aligned} \hat{H}_S = & \sum_{i,\sigma} (\epsilon_i - \mu_i) c_{i\sigma}^\dagger c_{i\sigma} + \sum_{i \neq j, \sigma} t_{ij} c_{i\sigma}^\dagger c_{j\sigma} \\ & + \sum_i \Delta_i (c_{i\downarrow}^\dagger c_{i\uparrow}^\dagger + c_{i\uparrow} c_{i\downarrow}), \end{aligned} \quad (2)$$

where Δ_i is the local superconducting order parameter.

Within this model, the coupling between the N (F) and S regions is introduced by means of hopping elements connecting sites on both sides of the interface. By choosing appropriately the hopping elements on the different regions one can model different situations and in particular to control the transparency of the interface (for instance, taking $t_{ij} = t$ everywhere would correspond to the ideal interface). Disorder caused by static impurities can be modeled by a random distribution of the site energies $\epsilon_{i,\sigma}$.

For the theoretical description of a system containing superconductors it is useful to introduce the Nambu representation,¹⁶ which is given in terms of the two-component spinors $\hat{\psi}_i$ and $\hat{\psi}_i^\dagger$ given by

$$\hat{\psi}_i = \begin{pmatrix} c_{i\uparrow} \\ c_{i\downarrow}^\dagger \end{pmatrix}, \quad \hat{\psi}_i^\dagger = \begin{pmatrix} c_{i\uparrow}^\dagger & c_{i\downarrow} \end{pmatrix}. \quad (3)$$

The Nambu representation is adequate to describe a non-magnetic situation. Although it conventionally assigns spin up to the electron and spin down to the hole components, this choice is irrelevant in the case of spin degeneracy. For a magnetic case one would need to introduce, in principle, two extra components namely for an electron with spin down and

a hole with spin up. However, when the magnetism is introduced by means of a diagonal exchange field, symmetry relations between the propagators for electrons and holes (see below) make it possible to restrict the analysis to the usual Nambu space.

In terms of these operators the generic Hamiltonian can be written as

$$\hat{H} = \sum_{i,j} \hat{\psi}_i^\dagger \mathcal{H}_{ij} \hat{\psi}_j, \quad (4)$$

where

$$\mathcal{H}_{ij} = \delta_{ij} \begin{pmatrix} \epsilon_{i\uparrow} - \mu & \Delta_i \\ \Delta_i & -\epsilon_{i\downarrow} + \mu \end{pmatrix} + (1 - \delta_{ij}) \begin{pmatrix} t_{ij} & 0 \\ 0 & -t_{ij}^* \end{pmatrix}. \quad (5)$$

Although in principle one could choose an arbitrary lattice structure, we shall adopt the simple cubic lattice for the sake of simplicity.

III. ANALYSIS OF 1D N - S AND F - S STRUCTURES

As a starting point it is instructive to analyze simple one dimensional models for N - S and F - S structures. These examples would also allow to introduce the Green function formalism adapted to deal with superconducting and/or ferromagnetic correlations. The retarded and advanced frequency-dependent Green functions in the Nambu representation are defined as

$$\hat{G}_{ij}^{r,a}(\omega) = \mp \int dt e^{i\omega\tau} \theta(\pm\tau) \langle [\hat{\psi}_i(\tau), \hat{\psi}_j^\dagger(0)]_{\pm} \rangle. \quad (6)$$

In this definition, $\hat{G}_{ij,11}$ corresponds to the propagation of an up spin electron, while $\hat{G}_{ij,22}$ describe the propagation of a down spin hole. The remaining propagators can be obtained from the previous ones by simple relations. Thus, the propagator for down spin electrons is given by $-\hat{G}_{ij,22}^*(-\omega)$ while the one for up spin holes is equal to $-\hat{G}_{ij,11}^*(-\omega)$.

Within our local description we associate a finite N or F region with a linear chain of N sites coupled to a semi-infinite chain corresponding to the superconducting region. The sites on the N (F) region are labeled by 1 to N , where N denotes the site connected to the superconductor. The hopping element between neighboring sites is taken as t everywhere except at the interface, where it is denoted by t_c . Taking the coupling between the N (F) and the S regions as a perturbation the retarded (advanced) frequency-dependent Green functions of the coupled system in a Nambu representation can be obtained from the Dyson equation

$$\hat{G}^{r,a} = \hat{g}^{r,a} + \hat{g}^{r,a} \hat{V} \hat{G}^{r,a}, \quad (7)$$

where $\hat{g}^{r,a}$ are the retarded (advanced) Green functions of the uncoupled regions and \hat{V} is the term coupling both regions.

The Green functions on the outermost site of the N (F) region are then given by

$$\hat{G}_{11} = \frac{1}{D} \begin{pmatrix} g_{11}^\uparrow D + t_c^2 g_{1N}^\uparrow g_{N1}^\uparrow (g - t_c^2 g_{NN}^\downarrow d) & -t_c^2 g_{1N}^\uparrow g_{N1}^\downarrow f \\ -t_c^2 g_{1N}^\uparrow g_{N1}^\downarrow f & g_{11}^\downarrow D + t_c^2 g_{1N}^\downarrow g_{N1}^\downarrow (g - t_c^2 g_{NN}^\uparrow d) \end{pmatrix}, \quad (8)$$

where g and f are the diagonal and nondiagonal Green functions on the outermost site of the uncoupled superconductor (see Appendix A), $d = g^2 - f^2$, $g_{ij}^{\uparrow,\downarrow}$ are the electron propagators for up and down spins in the uncoupled N (F) region (see Appendix B) and

$$D = 1 - t_c^2 g (g_{NN}^\uparrow + g_{NN}^\downarrow) + t_c^4 d g_{NN}^\uparrow g_{NN}^\downarrow.$$

The condition $D(\omega) = 0$ determines the position of the Andreev states inside the superconducting gap. This condition can be further simplified taking into account that $\omega \sim \Delta \ll |t|$, which allows one to approximate g and f in the usual BCS-like form, i.e., $g(\omega) = -\omega/(t\sqrt{\Delta^2 - \omega^2})$ and $f(\omega) = \Delta/(t\sqrt{\Delta^2 - \omega^2})$. In this case the position of the Andreev states can be obtained from the following equation:

$$\frac{\omega}{\sqrt{\Delta^2 - \omega^2}} = \frac{\beta^2 \sin(N\phi_\uparrow) \sin(N\phi_\downarrow) - \sin[(N+1)\phi_\uparrow] \sin[(N+1)\phi_\downarrow]}{\beta [\sin(N\phi_\uparrow) \sin[(N+1)\phi_\downarrow] + \sin(N\phi_\downarrow) \sin[(N+1)\phi_\uparrow]}}, \quad (9)$$

where $\beta = (t_c/t)^2$ and $\phi_\sigma = \arccos(\omega - \epsilon_\sigma)/2t$. In the N - S case ($g^\uparrow = g^\downarrow$), the condition for the Andreev states adopts a more simple form:

$$\omega = \pm \Delta \frac{\beta^2 \sin^2(N\phi) - \sin^2[(N+1)\phi]}{\beta^2 \sin^2(N\phi) + \sin^2[(N+1)\phi]}. \quad (10)$$

The number of states inside the superconducting gap increases with the length of the normal region, at a typical rate of a new state when the length is increased by five times the superconducting coherence length $\xi_0 = 2ta/\pi\Delta$, where a is the lattice spacing. This behavior is illustrated in Fig. 2(a) for the case of a perfect interface ($t = t_c$). As can be observed, the states gradually move from the gap edges towards the Fermi energy. The states closer to the Fermi energy define a ‘‘minigap’’ whose value for large N behaves as $E_g \sim \pi t/4N$.

The transition from the normal to the ferromagnetic case can be studied as a function of the exchange field E_{ex} . As can be observed in Figs. 2(b), 2(c), and 2(d), the behavior of the Andreev states is significantly modified for increasing E_{ex} . In contrast to the N - S case where the states are symmetrically located with respect to the Fermi energy, in the F - S case there is an increasing asymmetry for increasing E_{ex} . The electron states corresponding to the majority (minority) spins emerge from the gap edges and move with increasing length towards $E_F + E_{\text{ex}}/2$ ($E_F - E_{\text{ex}}/2$), thus eventually crossing the Fermi level. Notice that, when E_{ex} becomes larger than 2Δ only states coming from the lower (upper) gap edge populate the gap for the majority (minority) spins.

The crossing of the Andreev states through the Fermi level takes place when the length is increased by five times $\xi_F = 2ta/\pi E_{\text{ex}}$ approximately and has important physical consequences: it gives rise to a change in the sign of the induced pairing amplitude given by

$$\langle c_{i\downarrow} c_{i\uparrow} \rangle = \frac{1}{\pi} \int_{-\infty}^{E_F} \text{Im}(G_{ii}^a)_{12}(\omega) d\omega. \quad (11)$$

The behavior of the induced pairing amplitude for increasing length is depicted in Fig. 3 for different values of the exchange field. Some features are worth noticing. In the first place, the above commented crossing gives rise to oscillations of the order parameter with a typical wavelength of the order of ξ_F . However, the overall decay length can be significantly larger since it is given by ξ_0 as in the N - S case. As we will show in Sec. IV, this qualitative behavior is still found in 3D systems and is consistent with the available experimental evidence.

For the sake of comparison, we also show in Fig. 3(d) the spatial variation of the induced pairing amplitude as a function of the distance from the interface in an infinite 1D F - S structure. A similar albeit smoother oscillatory behavior is found as compared to the previous case where the thickness is increased.

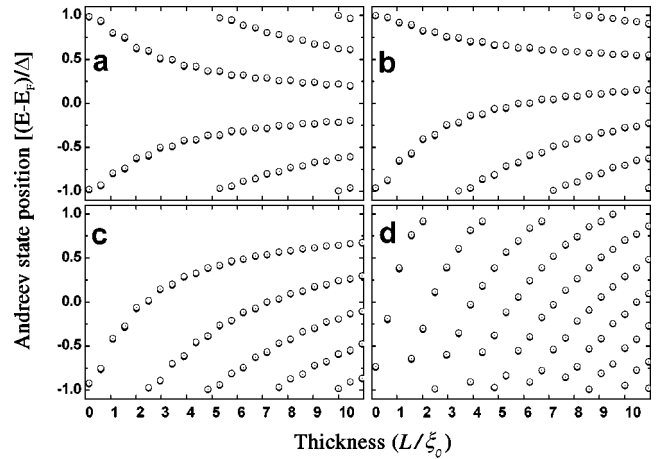


FIG. 2. Position of Andreev states in the spectral density for the majority spins as a function of the length of the F region within the 1D model described in the text. Cases (a)–(d) correspond to $E_{\text{ex}}/\Delta = 0, 0.8, 2,$ and 6 , respectively. The spectral density for the minority spins is obtained by specular reflection with respect to the Fermi energy.

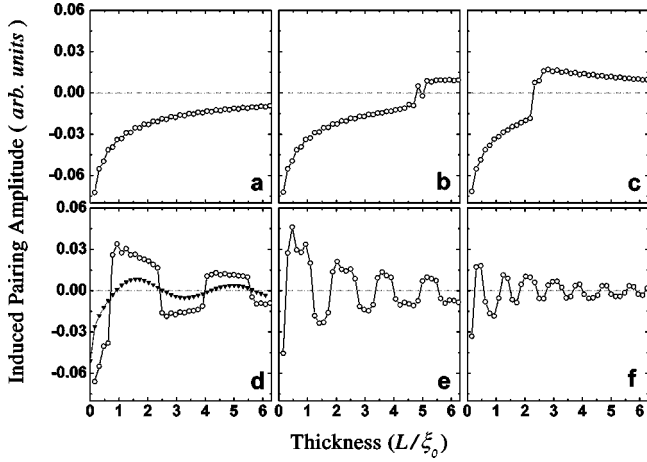


FIG. 3. Induced pairing amplitude on the surface of 1D F - S structure as a function of the F region thickness (in units ξ_0). Cases (a)–(f) correspond to increasing values of the exchange field parameter $E_{\text{ex}}/\Delta = 0, 1, 2, 6, 12,$ and 18 . In case d the triangles correspond to the spatial variation of the induced pairing amplitude as function of the distance to the interface in an infinite F - S structure.

IV. RECURSION METHOD

We present in this section a generalization of the recursion method¹³ for the calculation of the local electronic properties in nonhomogeneous superconducting 3D structures. In the normal version, the recursion method consists in the recursive construction of an orthogonal basis in which the Hamiltonian adopts a tridiagonal form. The first state in this basis is taken at the site where the local density of states is to be calculated, i.e., $|v_1\rangle = |0\rangle$. Then, the states in the new basis are generated by the recursive equations

$$\begin{aligned} b_1|v_2\rangle &= H|v_1\rangle - a_1|v_1\rangle, \\ b_2|v_3\rangle &= H|v_2\rangle - a_2|v_2\rangle - b_1|v_1\rangle, \dots, \\ b_n|v_{n+1}\rangle &= H|v_n\rangle - a_n|v_n\rangle - b_{n-1}|v_{n-1}\rangle, \dots, \end{aligned} \quad (12)$$

where the coefficients a_n, b_n are determined by the orthogonality condition between the states $|v_n\rangle$ and correspond to the diagonal and non-diagonal elements of the Hamiltonian in the new representation. This method thus defines a mapping into an effective semi-infinite one-dimensional chain in which the local Green functions can be evaluated as a continued fraction given by

$$\begin{aligned} G_{00}(\omega) &= [\omega - a_1 - b_1^2 g_1(\omega)]^{-1}, \\ g_1(\omega) &= [\omega - a_2 - b_2^2 g_2(\omega)]^{-1} \dots, \\ g_{n-1}(\omega) &= [\omega - a_n - b_n^2 g_n(\omega)]^{-1} \dots \end{aligned} \quad (13)$$

The extension of the recursion method to deal with nonhomogeneous superconductors is not straightforward. To begin with, there is not a unique way of constructing this generalization. In an earlier attempt, Litak *et al.*¹⁵ proposed a generalization in which two recursion basis are constructed starting from electron and hole like states. However, the

2×2 structure of the Nambu space suggests that one could develop a single recursion procedure by introducing a basis transformation with 2×2 matrix coefficients.

We begin by rewriting Hamiltonian (4) in a 2×2 Nambu matrix form

$$\hat{H} = \sum_i \begin{pmatrix} \epsilon_{i\uparrow} & \Delta_i \\ \Delta_i & -\epsilon_{i\downarrow} \end{pmatrix} |\mathbf{i}\rangle\langle\mathbf{i}| + \sum_{ij} \begin{pmatrix} t_{ij} & 0 \\ 0 & -t_{ij}^* \end{pmatrix} |\mathbf{i}\rangle\langle\mathbf{j}|, \quad (14)$$

where $|\mathbf{i}\rangle\langle\mathbf{j}|$ are projection operators in the site space which do not operate in the Nambu space. A general basis can be written in terms of the site basis $\{|\mathbf{i}\rangle\}$ as

$$|\mathbf{v}_n\rangle = \sum_i \begin{pmatrix} v_{n,i}^{11} & v_{n,i}^{12} \\ v_{n,i}^{21} & v_{n,i}^{22} \end{pmatrix} |\mathbf{i}\rangle. \quad (15)$$

The orthogonality condition between two states $|\mathbf{v}_n\rangle, |\mathbf{v}_m\rangle$ impose four conditions on their coefficients given by

$$\sum_{i,\gamma} v_{n,i}^{\alpha\gamma} v_{m,i}^{\gamma\beta} = \delta_{nm} \delta_{\alpha\beta}. \quad (16)$$

In order to generate the local Green functions (both the diagonal and nondiagonal components in Nambu space) at a site denoted by 0, the initial state in the recursive procedure is taken as

$$|\mathbf{v}_1\rangle = \begin{pmatrix} 1 & 0 \\ 0 & 1 \end{pmatrix} |\mathbf{0}\rangle. \quad (17)$$

In the generalization of the recursive equations (12) to the superconducting case the coefficients a_n and b_n become 2×2 matrices \hat{a}_n, \hat{b}_n . One should then take care of the non-commuting nature of matrix algebra in writing the new equations which turn out to be given by

$$\begin{aligned} |\mathbf{v}_2\rangle \hat{b}_1 &= \hat{H}|\mathbf{v}_1\rangle - |\mathbf{v}_1\rangle \hat{a}_1, \\ |\mathbf{v}_3\rangle \hat{b}_2 &= \hat{H}|\mathbf{v}_2\rangle - |\mathbf{v}_2\rangle \hat{a}_2 - |\mathbf{v}_1\rangle \hat{b}_1 \dots, \\ |\mathbf{v}_{n+1}\rangle \hat{b}_n &= \hat{H}|\mathbf{v}_n\rangle - |\mathbf{v}_n\rangle \hat{a}_n - |\mathbf{v}_{n-1}\rangle \hat{b}_{n-1} \dots \end{aligned} \quad (18)$$

As in the normal case, the matrix coefficients \hat{a}_n and \hat{b}_n are determined by the orthogonality conditions between consecutive states in the new basis. Thus, \hat{a}_n is obtained trivially from the last equation by taking the scalar product with the state $|\mathbf{v}_n\rangle$, leading to $\hat{a}_n = \langle \mathbf{v}_n | \hat{H} | \mathbf{v}_n \rangle$. On the other hand, the orthogonality conditions only permits one to determine $\hat{b}_n^\dagger \hat{b}_n$ leading to an intrinsic ambiguity in the determination of \hat{b}_n as we discuss below. Notice that $\hat{b}_n^\dagger \hat{b}_n$ is calculated from the scalar product of the state $|\tilde{\mathbf{v}}_n\rangle = |\mathbf{v}_n\rangle \hat{b}_n$ with itself.

In the nonmagnetic case it can be shown that the state $|\tilde{\mathbf{v}}_n\rangle$, which is obtained by successive application of the Hamiltonian to the initial state, have components which are symmetric matrices of the form

$$\langle \mathbf{i} | \tilde{\mathbf{v}}_n \rangle = \begin{pmatrix} \alpha_{ni} & \beta_{ni} \\ \beta_{ni} & -\alpha_{ni} \end{pmatrix}. \quad (19)$$

Thus, $\hat{b}_n^\dagger \hat{b}_n$ is a diagonal matrix from which the coefficients \hat{b}_n are directly extracted by taking the square root. There is an ambiguity in the election of the sign of the square root. However, this choice does not affect the physical quantities such as the local densities of states. Since the diagonal elements of the matrix \hat{b}_n can be interpreted as the hopping elements of an effective one-dimensional model, we choose $(\hat{b}_n)_{11} = -(\hat{b}_n)_{22}$ as in the hopping matrix of the initial Hamiltonian in the Nambu representation.

In the magnetic case the above commented symmetry in the components of $|\tilde{\mathbf{v}}_n\rangle$ is lost. In this case $\hat{b}_n^\dagger \hat{b}_n$ is no longer a diagonal matrix and, as a consequence, the matrix coefficients \hat{b}_n can acquire nondiagonal elements. To obtain these coefficients the matrix $\hat{b}_n^\dagger \hat{b}_n$ is first diagonalized and then transformed back to the original basis after taking the square root.

Once the coefficients \hat{a}_n and \hat{b}_n are determined, it is straightforward to obtain the local Green function matrix \hat{G}_{00} by evaluating the matrix continued fraction

$$\begin{aligned} \hat{G}_{00}(\omega) &= [\omega \hat{I} - \hat{a}_1 - \hat{b}_1^\dagger \hat{g}_1(\omega) \hat{b}_1]^{-1}, \\ \hat{g}_1(\omega) &= [\omega \hat{I} - \hat{a}_2 - \hat{b}_2^\dagger \hat{g}_2(\omega) \hat{b}_2]^{-1} \dots, \\ \hat{g}_{n-1}(\omega) &= [\omega \hat{I} - \hat{a}_n - \hat{b}_n^\dagger \hat{g}_n(\omega) \hat{b}_n]^{-1} \dots. \end{aligned} \quad (20)$$

One should finally devote some consideration to the problem of the truncation of the continued fraction. In practice, one can only calculate exactly a finite number of coefficients. In most cases a convergence into certain limiting coefficients $\hat{a}_\infty, \hat{b}_\infty$ is observed for a sufficiently large number of iterations. In that case the continued fraction can be terminated using the constant termination procedure, which is well known for the normal case.¹⁷ In the superconducting case the equivalent procedure requires to obtain the local Green function for a semi-infinite homogeneous superconducting chain (see Appendix A).

However, in certain situations which involve localized states inside the superconducting gap, the coefficients can exhibit aperiodic long range oscillations. Nevertheless, it can be shown that the local densities of states converge for sufficiently large number of iterations even when the individual coefficients do not tend to an asymptotic value.

In order to illustrate the accuracy of the method we have calculated the subgap local density of states (LDOS) for a N - S 1D example where the exact result can be obtained by solving the Dyson equation as in the previous section. The results in Fig. 4 exhibit the convergence into the exact solution as the number of iterations is increased.

V. 3D N - S AND F - S NANOSTRUCTURES

We are interested in analyzing how the distribution of Andreev states evolves as the lateral dimensions of a N - S or

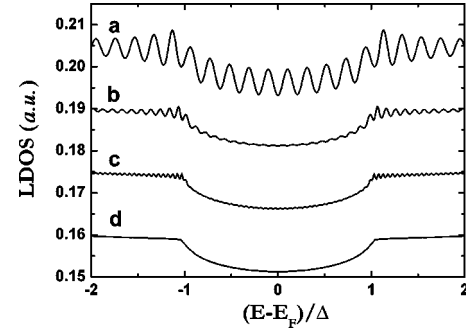


FIG. 4. LDOS on a site at the interface in an infinite 1D N - S structure. Cases (a), (b), and (c) are obtained using the generalized recursion method with 300, 600, and 1200 recursion steps while (d) corresponds to the exact result obtained by solving the Dyson equation.

a F - S structure increase from the 1D to the infinite planar junction case. For analyzing this transition we have considered a prismatic geometry such as the one depicted in Fig. 1, in which the cross section is varied by changing the number M of sites on the square side.

It should be noticed that the case of a ballistic normal layer on top of a superconductor was first analyzed by de Gennes and Saint-James¹⁸ who showed that the Andreev states form a continuous band filling the gap region. They found that the density of states around the Fermi energy behaves as $\sim |\omega|$ for arbitrary thickness.

In Fig. 5 we analyze the transition in the LDOS at the surface of the normal region, from the 1D to the infinite planar geometry. As can be observed, the subgap LDOS evolves from a single localized Andreev peak in the 1D case to a continuous LDOS in the infinite lateral dimension limit. As the lateral dimension is increased the subgap states tend to group themselves into a bunch located at the position of the original 1D state with a tail which gradually fills the gap.

As can be observed in Fig. 6, for lateral dimensions of the order of a few times ξ_0 the LDOS can be hardly distin-

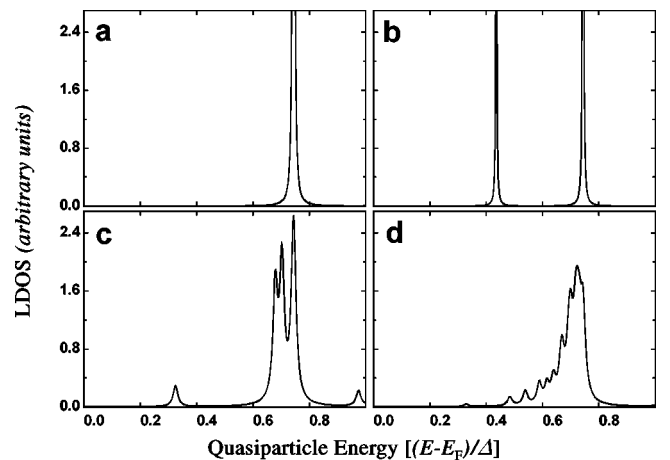


FIG. 5. Evolution of the surface subgap LDOS on a 3D N - S structure when increasing the lateral dimensions. The normal layer thickness is $1.56 \xi_0$. Cases (a) to (d) correspond to a lateral width equal to $0.156, 0.78, 1.404,$ and $3.276 \xi_0$, respectively.

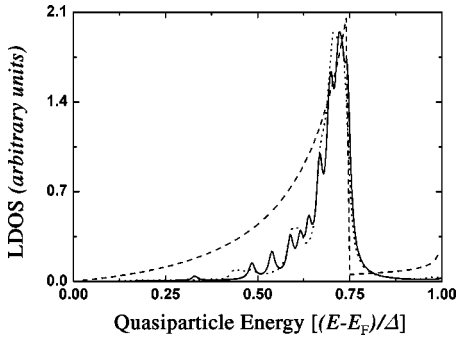


FIG. 6. Surface subgap LDOS of case (d) in Fig. 5 compared to the infinite width limit (dotted line) and the corresponding result of the de Gennes–Saint-James theory (dashed line).

guished from the infinite planar geometry limit except for some minor structure (in this limit the problem becomes diagonal in the parallel wave vector representation: the corresponding LDOS can then be evaluated by direct summation over this component of the wave vector). When comparing the LDOS in the infinite planar limit with the result of the de Gennes and Saint-James model (see Fig. 6) several differences become apparent. The most important one is the absence of a linear DOS around the Fermi energy. This is basically due to the fact that the de Gennes–Saint-James calculation corresponds to the *total* DOS of the normal region instead of just the surface LDOS. On the other hand, the LDOS in the lattice model does not exhibit an abrupt jump at the position of the 1D Andreev states as is in the de Gennes–Saint-James result. This difference is due to the finite value of the parameter Δ/t , which invalidates the Andreev approximation, and the deviation from a parabolic energy-momentum relation in the perpendicular direction for certain values of the parallel wave vector. In this sense both models are not completely equivalent.

It is important to notice that in a tunneling experiment the measured quantity is the surface LDOS instead of the total normal region DOS. Therefore, the linear behavior around the Fermi energy predicted by de Gennes–Saint-James would not be observed even in the ideal ballistic case.¹⁹ In contrast our results predict a much faster decay. As a consequence, the distinction between the ballistic and the diffusive case (in which a minigap is predicted to appear²⁰) could be difficult to observe experimentally.

A similar analysis for the transition from 1D to the infinite planar limit can be performed for the F - S case. As in the case of N - S structures it is found that the 1D features are robust, i.e., the LDOS exhibits pronounced peaks around the position of the original 1D states with tails gradually filling the gap. The surface LDOS corresponding to the infinite planar limit is shown in Fig. 7 for different values of the exchange field parameter. While for $E_{\text{ex}} \sim \Delta$ the spectrum is still similar to the N - S case but with a slight e-h asymmetry, for much larger values of E_{ex} the LDOS exhibits a much more complex structure distributed quite evenly inside the gap.

Spatial behavior of the LDOS and induced pairing amplitude in 3D F - S structures. Let us now analyze the spatial behavior of the induced pairing amplitude and LDOS in a 3D

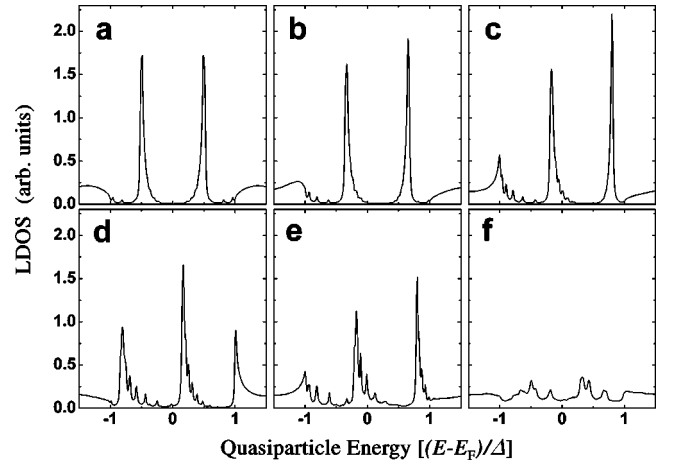


FIG. 7. Majority spin surface subgap LDOS for a F - S structure in the infinite width limit for different values of the exchange field parameter. Cases (a)–(f) correspond to $E_{\text{ex}}/\Delta = 0, 0.5, 1, 2, 4,$ and 20 .

F - S structure. It is possible to conceive two types of experiments for testing these quantities: in one case the LDOS is measured for increasing thickness of the F region; while in the other the spatial behavior would be scanned along the surface at increasing distances from the interface for a given thickness. So far, experiments have probed the evolution of the LDOS with the size of the F region in F - S layers.⁵ An oscillatory behavior of the induced pairing amplitude was observed. A more detailed comparison with the theory would require using the second method, which could be implemented by means of the scanning tunneling microscope.

The spatial behavior of the LDOS for a F - S nanostructure is shown in Fig. 8. We have chosen an exchange field parameter $E_{\text{ex}} \sim 6\Delta$, which is close to the experimental situation in Ref. 5. As can be observed, the most significant features are due to the evolution of the 1D Andreev states, which origi-

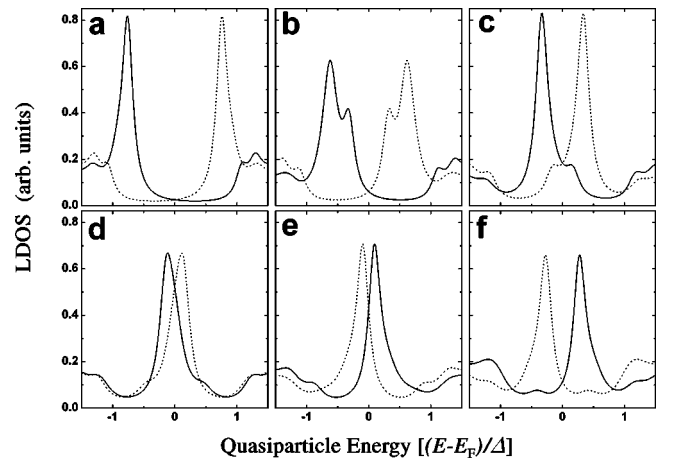


FIG. 8. Majority spin (full line) and minority spin (dotted line) surface subgap LDOS on a F - S nanostructure in the infinite width limit as a function of the F layer thickness, L . Cases (a)–(f) correspond to $L/\xi_F = 0.94, 1.88, 2.83, 4.24, 5.31, 6.37$. A smaller energy resolution has been used in order to stress the main features of the subgap LDOS.

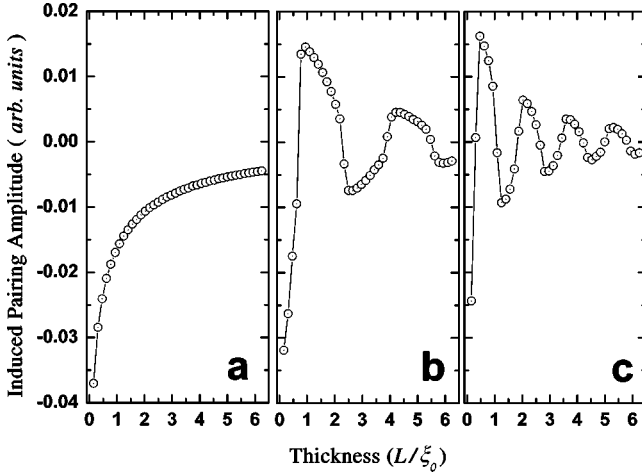


FIG. 9. Induced pairing amplitude on the surface of 3D F - S structure as a function of the F region thickness (in units ξ_0). The lateral width is equal to $L/\xi_0 = 7.66$ which, with the actual choice of parameters, corresponds to a 49×49 sites in the cross section. Cases (a), (b), and (c) correspond to $E_{\text{ex}}/\Delta = 0, 6,$ and 12 .

nate at the gap edges, move towards the center and eventually cross the Fermi energy. This evolution gives rise to an oscillatory sequence of peaks and valleys around the Fermi energy. Although this behavior is in qualitative agreement with the results of Ref. 5, the present theory corresponds to a much larger spatial resolution which cannot be reached in this type of experiment.

As commented in the 1D case, this crossing of Andreev states leads also to a spatial oscillatory behavior of the induced pairing amplitude, as illustrated in Fig. 9. Although the overall qualitative behavior is similar to the one found in 1D, the amplitude of the oscillations are reduced by a factor of the order of 3. A similar oscillatory behavior would be obtained when the induced pairing amplitude is scanned as a function of the distance to the interface in an infinite F - S structure.

VI. CONCLUSIONS

A generalized recursion method for the calculation of the local spectral densities in hybrid N - S and F - S nanostructures has been presented. This method allows one to study the proximity effect in structures of arbitrary geometry.

Using this method we have made a detailed analysis of the spatial variation of the spectral densities and the induced pairing amplitude in the region close to the interface in ballistic N - S and F - S structures. We have shown that the simplest 1D models already contain the essential ingredients which determine this spatial variation, namely, the evolution of the Andreev states inside the superconducting gap as a function of the N or F region size. In the F - S case it has been shown that the oscillations at the scale of ξ_F in the induced pairing amplitude and in the LDOS at the Fermi energy can be correlated to the evolution of the Andreev states inside the gap. These oscillations exhibit an overall decay length significantly larger than ξ_F , which is controlled by ξ_0 as in the N - S case. We believe that this is an interesting result since

the typical length for proximity effect in F - S systems is currently under debate.³⁻⁶

Although the present results are consistent with the available experimental data, this theoretical analysis would become more relevant in connection with new experiments using local probes such as the scanning tunneling microscope which would provide larger spatial and energy resolution. Experiments along these lines are starting to be developed.²¹

ACKNOWLEDGMENTS

The authors would like to thank A. Martin for useful comments on the recursion method. This work has been supported by the Spanish CICYT under Contract No. PB97-0044.

APPENDIX A

In this appendix we obtain the expressions for the diagonal and nondiagonal (in Nambu space) Green functions in the outermost site of an homogeneous semi-infinite superconducting chain. From the Dyson equation (7) it can be shown that these quantities satisfy the matrix equation

$$[\omega \hat{l} - \hat{h}_0 - \hat{t} \hat{g} \hat{t}] \hat{g} = \hat{l}, \quad (\text{A1})$$

where

$$\hat{h}_0 = \begin{pmatrix} \epsilon - \mu & \Delta \\ \Delta & -(\epsilon - \mu) \end{pmatrix}, \quad \hat{t} = \begin{pmatrix} t & 0 \\ 0 & -t \end{pmatrix}.$$

In the case of electron-hole symmetry $\epsilon - \mu = 0$ and $g_{11} = g_{22} = g$ while $g_{12} = g_{21} = f$. Then, Eq. (A1) can be easily solved yielding for the advanced component

$$g(\omega) = \frac{\omega}{2t^2} \left[1 - \sqrt{\frac{\omega^2 - 4t^2 - \Delta^2}{\omega^2 - \Delta^2}} \right]$$

$$\text{for } |\omega| < \Delta \quad \text{or} \quad |\omega| > \sqrt{4t^2 + \Delta^2},$$

$$g(\omega) = \frac{\omega}{2t^2} \left[1 + i \operatorname{sgn}(\omega) \sqrt{\frac{4t^2 + \Delta^2 - \omega^2}{\omega^2 - \Delta^2}} \right]$$

$$\text{for } \Delta < |\omega| < \sqrt{4t^2 + \Delta^2}. \quad (\text{A2})$$

The nondiagonal Green function is simply given by $f(\omega) = -\Delta g(\omega)/\omega$.

APPENDIX B

In this appendix we obtain the electron propagators for a finite ferromagnetic 1D chain having N sites. The Green functions for the up or down spins g_{1n}^σ , where 1 denotes the outermost site of the chain and $1 \leq n \leq N$, can be obtained from the propagators of a semi-infinite homogeneous 1D chain \tilde{g}_{1n}^σ by introducing a perturbation which decouples the outermost N sites from the rest of the chain. We first notice that \tilde{g}_{1n}^σ can be expressed in terms of a phase factor in the form

$$\tilde{g}_{1n}^{\sigma} = \frac{e^{in\phi_{\sigma}}}{t}, \quad (\text{B1})$$

where $\phi_{\sigma} = \arccos(\omega - \epsilon_{\sigma})/2t$. Solving the Dyson equation for a perturbation corresponding to subtracting the bond be-

tween the N and $N+1$ sites one readily obtains

$$g_{1n}^{\sigma} = \frac{1}{t} \frac{\sin[(N-n+1)\phi_{\sigma}]}{\sin[(N+1)\phi_{\sigma}]}. \quad (\text{B2})$$

-
- ¹G. Deutscher and P.G. de Gennes, in *Superconductivity*, edited by R.D. Parks (M. Dekker, New York, 1969), p. 1005.
- ²S. Guéron, H. Pothier, Norman O. Birge, D. Esteve, and M. H. Devoret, *Phys. Rev. Lett.* **77**, 3025 (1996).
- ³J. Aarts, J. M. E. Geers, E. Brúć, A. A. Golubov, and R. Coehoorn, *Phys. Rev. B* **56**, 2779 (1997).
- ⁴M. Giroud, H. Courtois, K. Hasselbach, D. Mailly, and B. Pannetier, *Phys. Rev. B* **58**, R11 872 (1998).
- ⁵T. Kontos, M. Aprili, J. Lesueur, and X. Grison, *Phys. Rev. Lett.* **86**, 304 (2001).
- ⁶J. Aumentado and V. Chandrasekhar, *Phys. Rev. B* **64**, 054505 (2001).
- ⁷L. Usadel, *Phys. Rev. Lett.* **95**, 507 (1970).
- ⁸M. Zareyan, W. Belzig, and Yu. V. Nazarov, *Phys. Rev. Lett.* **86**, 308 (2001).
- ⁹A. Martín-Rodero, F. J. García-Vidal, and A. Levy Yeyati, *Phys. Rev. Lett.* **72**, 554 (1994).
- ¹⁰A. Levy Yeyati, A. Martín-Rodero, and F. J. García-Vidal, *Phys. Rev. B* **51**, 3743 (1995).
- ¹¹A. Levy Yeyati, J. C. Cuevas, A. López-Dávalos, and A. Martín-Rodero, *Phys. Rev. B* **55**, R6137 (1997).
- ¹²*The Hubbard Model: A Reprint Volume*, edited by A. Montorsi (World Scientific, Singapore, 1992).
- ¹³R. Haydock, V. Heine, and M. J. Kelly, *J. Phys. C* **5**, 2845 (1972).
- ¹⁴See, for instance, various articles in *The Recursion Method and its Applications*, edited by D. G. Pettiford and D. L. Weaire (Springer-Verlag, Berlin, 1985).
- ¹⁵G. Litak, P. Miller, and B. L. Gyorffy, *Physica C* **251**, 263 (1995).
- ¹⁶Y. Nambu, *Phys. Rev.* **117**, 648 (1960).
- ¹⁷A. Trías, M. Kiwi, and M. Weissmann, *Phys. Rev. B* **28**, 1859 (1983).
- ¹⁸P. G. de Gennes and D. Saint-James, *Phys. Lett.* **4**, 151 (1963).
- ¹⁹The discrepancy between the DOS calculated by de Gennes and Saint-James and experimental results was pointed out long ago. See, e.g., J. Bar-Sagi, *Solid State Commun.* **15**, 729 (1974).
- ²⁰W. Belzig, C. Bruder, and G. Schön, *Phys. Rev. B* **54**, 9443 (1996).
- ²¹N. Moussy, H. Courtois, and B. Pannetier, *Rev. Sci. Instrum.* **72**, 128 (2001).